Small-Angle Neutron Scattering Studies on Thin Films of Isotopic Polystyrene Blends

D. L. Ho and R. M. Briber*

Materials and Nuclear Engineering Department, 2100 Marie Mount Hall, University of Maryland, College Park, Maryland 20742

R. L. Jones and S. K. Kumar

Department of Materials Science and Engineering, Pennsylvania State University, University Park, Pennsylvania 16802

T. P. Russell

Department of Polymer Science and Engineering, University of Massachusetts, Amherst, Massachusetts 01003

Received May 7, 1998; Revised Manuscript Received July 20, 1998

ABSTRACT: Thin films of various thicknesses ranging from 100 μm down to 1390 Å of an isotopic polystyrene blend were examined using small-angle neutron scattering. It was found that absolute scattering data with reasonable signal-to-noise could be obtained from single films as thin as 1390 Å supported on single-crystal Si wafers by optimizing the neutron optics and by carefully eliminating background arising from the substrate. The wave vector dependence of the neutron scattering from all of the films examined could be described using the random phase approximation with the same Flory−Huggins interaction parameter and R_G values as found in the bulk. No dependence of the scattering on film thickness was found. These results demonstrate that quantitative small-angle neutron scattering measurements can be obtained from single ultrathin films of polymer mixtures.

Introduction

In recent years small-angle neutron scattering (SANS) has been widely used to characterize the thermodynamics of polymer mixtures.[1−3] These studies have generally focused on bulk samples due to the limited neutron flux available at most sources. However, Russell et al.[4] have recently utilized SANS to qualitatively study the structure of films of block copolymers and polymer mixtures with thicknesses as small as 1000 Å. Block copolymers of polystyrene (PSH) and deuterated poly(methyl methacrylate) (dPMMA) and homopolymer blends of PSH and deuterated polystyrene (PSD) were investigated in their experiments. All of the thin-film samples were prepared by spin coating films onto silicon single-crystal substrates. For the PSD ($M_w \sim 760$ K g/mol)/PSH ($M_w \sim 690$ K g/mol) homopolymer blends the experiments were performed on a ∼1700 Å thick thin film of a 50/50 mixture. SANS was measured for the as-spun film and after annealing at 130 °C for 15 h. The data for the as-spun film were fit to a Debye scattering function which yielded a radius of gyration, $R_G = 470 \pm 50$ Å, and $I(0) = 2000 \pm 500$ cm^{-1}. For the annealed film an $R_G = 1900 \pm 500$ Å and $I(0) = 54\,000 \pm 9000$ cm^{-1} were obtained. These values correspond to a Kuhn segment length of ∼56.5 Å and χ of $\sim 2.9 \times 10^{-4}$. The calculated values in the bulk for this blend (at 130 °C) are $I(0) = 2360$ cm^{-1}, $R_G = 230$ Å, $\chi = 2.1 \times 10^{-4}$, and $T_C = 67$ °C based on the work by Londono et al.[5] As discussed by Russell et al., the deviation from the bulk values, particularly for R_G of the as-spun film, could be due to the homopolymers being trapped in a nonequilibrium conformation during the spinning process. For the annealed film the very large values for $I(0)$ and R_G obtained suggest that the film is phase separated. Phase separation of the blend after annealing at 130 °C would indicate a large shift ($\Delta T_C \sim 60$ °C) in the upper critical solution temperature (UCST) phase boundary due to finite size effects. In an optical microscope study, Reich and Cohen[6] have found that the lower critical solution temperature (LCST) phase boundary for polystyrene and poly(vinyl methyl ether) (PVME) blends was observed to begin to shift significantly for films as thick as 1 μm (i.e., $\Delta T_C \sim 5$ °C) depending on the details of sample preparation. Substantially larger shifts were observed for thinner films ($\Delta T_C \sim 40$ °C for ~ 0.1 μm). The molecular weights used by Reich and Cohen were quite low (PS $M_W = 36\,000$ g/mol and PVME $M_W = 10\,700$ g/mol), indicating that finite size effects may be operative at film thicknesses 10^2 R_G or greater.

Recent theoretical calculations and simulations[7−10] have predicted that the miscibility of a polymer blend should be affected for film thicknesses less than the contour length of the chain. A polystyrene chain with a molecular weight of 10^5 g/mol has a contour length of approximately 0.3 μm. These experimental and theoretical results indicate that finite size effects may be found in films many times thicker than R_G. The range of differing results from both theory and experiments where both stabilization and destabilization have been observed led to the conclusion that additional SANS experiments on thin films of a model blend system (PSD/PSH) were needed to gain insight into this important issue. Prior to investigating the details of the phase diagram and changes in T_C for thin films, experimental work was required to develop the SANS technique to determine the limit of thickness for a single film where $I(0)$, R_G, and χ could be determined *quantitatively* using

* To whom correspondence should be addressed.

10.1021/ma980733s CCC: $15.00
Published on Web 12/04/1998

Table 1. Characteristics of the Homopolymers[a]

PSD: $M_w = 289\,000$	$M_w/M_n = 1.04$
PSH: $M_w = 284\,000$	$M_w/M_n = 1.05$

[a] PSD/PSH blend composition: 25/75 by weight.

current neutron sources. The ability to perform these thin-film experiments in normal transmission scattering geometry in a reasonable amount of time with a good signal-to-noise (S/N) ratio is based on the development of a liquid hydrogen cold neutron source[11] and the optimization of the collimation optics to maximize the neutron flux on the sample. The experiments also exploit the low absorption and (generally) negligible small-angle scattering of single-crystal silicon wafers for use as substrate materials. Although not discussed in this paper, grazing incidence small-angle scattering of neutrons has also been used for studying thin films and surfaces and is complementary to normal incidence scattering as it obtains information in the normal (*z*-axis) direction along with in-plane structure in one direction.[12−15]

In addition to testing the limits of SANS for the quantitative study of thin polymer blend films, this work will also examine the results found by Russell et al., where significant effects of confinement were found even when film thicknesses were $L/R_G \sim 9$.

Experimental Method and Data Analysis

The characteristics of the polystyrene homopolymers (obtained from Polymer Source, Inc.) used in these experiments are given in Table 1. Deuterated polystyrene (PSD)/protonated polystyrene (PSH) thin films of composition 25/75 PSD/PSH by weight were spun from toluene solutions onto 2.3 cm diameter silicon (Si) wafers (∼0.02 cm thick). It should be noted that a 2.3 cm diameter polystyrene thin film which is 2000 Å thick corresponds to a sample mass of only about 100 μg. Prior to spinning, the wafers were cleaned in chromerge at 80 °C for 3 h, etched using hydrofluoric (HF) acid, and thoroughly rinsed with deionized water. The spin-coated films on the Si wafers were annealed at 120 °C in a vacuum overnight and quenched to room temperature. PSD/PSH blends are known to have a UCST phase diagram due to the isotope effect.[16] For the polymer molecular weights and compositions studied in this work, a spinodal temperature of −125 °C is estimated based on published values of the H/D segmental interaction parameter, χ_{HD}.[5] It should be noted that the annealing temperature is more than 200 °C above the bulk spinodal temperature, and hence the films should be deep within the one-phase region of the phase diagram. The blend studied in this work was specifically chosen to be far from the phase boundary to minimize complications arising from phase separation and/or shifts in T_C, allowing the determination of the limits of the SANS technique for single-phase blends. In addition to the thin films, two bulk samples with thicknesses of 109 and 129 μm were prepared by melt pressing at 160 °C, annealed at 120 °C, and quenched to room temperature prior to the SANS measurements.

To generate absolute intensity SANS data from thin films, it is essential to obtain accurate measurements of the film thickness. Ellipsometry and X-ray reflectivity (XRR) were used for this purpose. Table 2 shows the measured film thicknesses as well as the average values used for data reduction. Samples will be denoted by their average thickness throughout the text of this paper.

SANS experiments were performed at room temperature using the 30 m NG3 and NG7 SANS instruments at the National Institute of Standards and Technology (NIST) Center for Neutron Research (NCNR)[17] with neutrons of wavelength $\lambda = 6$ Å, four guides, 10.8 m sample-to-detector distance, and wavelength resolution $\Delta\lambda/\lambda = 0.22$. Scattering was measured over the q range from 0.007 to 0.06 Å^{-1}. A large final

Table 2. Thickness Measurements (in Å)

nominal thickness	ellipsometry[a]	XRR[b]	thickness used
1000	1390 ± 25	1430	1390
2000	2340 ± 25	N/A	2340
4000	4270 ± 250	N/A	4270
7000	6960 ± 75	N/A	6960
9000	9170 ± 30	N/A	9170

[a] Errors reflect range in values determined by several measurements at different laboratories. [b] XRR: X-ray reflectivity.

collimation aperture (1.91 cm) was used for all samples to increase the neutron flux on the sample (and hence the S/N ratio), except for the two thinnest films where a 1.59 cm aperture was used due to defects on the edge of the Si wafers. Using these collimation optics, the neutron flux on the sample was approximately 1.2×10^6 neutrons/(cm^2 s). Due to the small amount of scattering being measured, all experiments were performed with the sample chamber under vacuum (∼0.2 Torr). With air in the sample chamber the count rate of the open beam (without any sample) would almost double, adding greatly to the background signal and making the experiments significantly more difficult for the thinnest samples. The data collection times ranged from 2 h for the thickest sample to 10 h for the thinnest. Transmission coefficients for all the thin-film samples were measured (and calculated) to be unity to within experimental error.[1,18]

The scattered intensities were corrected for background and parasitic scattering using standard means.[19] The data collection times for the blocked beam background and empty cell were comparable to that for the thinnest sample. The scattering from the open beam, indistinguishable from that of a single clean Si wafer, was used as the empty cell for data reduction. The data were placed on an absolute level using a calibrated secondary standard and were circularly averaged to yield the intensity, I, as a function of q where $q = (4\pi/\lambda)\sin(\theta/2)$ (θ is the scattering angle).

The ability to perform these SANS experiments is dependent on the Si wafer substrate being transparent to neutrons and not contributing significantly to the measured scattering. The Si(111) wafers used in this work (obtained from Semiconductor Processing) were grown by the Czochralski (CZ) method. Si-(111) wafers would not be suitable for experiments requiring stacking of multiple wafers using 6 Å wavelength neutrons due to double diffraction, which would give rise to Bragg diffraction and obscure the small-angle scattering region. Double diffraction can be avoided by increasing the neutron wavelength to greater than the Bragg cutoff of $2d$, where $d_{111} = 3.14$ Å for Si (111); however, the incident neutron flux decreases as λ^4 for a reactor neutron source. As an alternative to using (111) orientation wafers, a series of (100) wafers were tested as substrates. The lattice constant of Si (100) is $d_{100} = 5.43$ Å, which should allow stacking of samples using 6 Å neutrons as the Bragg diffraction angle is significantly less than 90° and should not cause problems with double diffraction in the forward direction. PSD/PSH films spun on the (100) orientation wafers exhibited scattering that is apparently characteristic of a phase-separated blend. Figure 1 shows Zimm plots ($I^{-1}(q)$ versus q^2) for ∼4000 Å thick films of PSD/PSH spin coated onto single Si(111) and Si(100) wafers. The SANS data from the (100) wafer show significantly enhanced scattering with a negative intercept, suggesting that the blend is phase separated. On the other hand, the data from the mixture on the Si(111) wafer indicates that the system is single phase. The origin of this discrepancy lies in the surface roughness of the wafers. Video-enhanced differential interference contrast (DIC) optical microscopy images (shown in Figure 2a,b) and atomic force microscopy (AFM) images (shown in Figure 3a,b) show that the surface of the Si(100) wafer is much rougher than that of the Si(111). (All wafers appeared highly polished to the eye.) The wavelength of the roughness is on the order of 1 μm while the peak-to-valley height is about 30 Å. AFM indicates that the roughness for the (111) wafer over a 1 μm wavelength is less than the noise level in the image of ±3 Å. Since the diffraction vector is oriented parallel

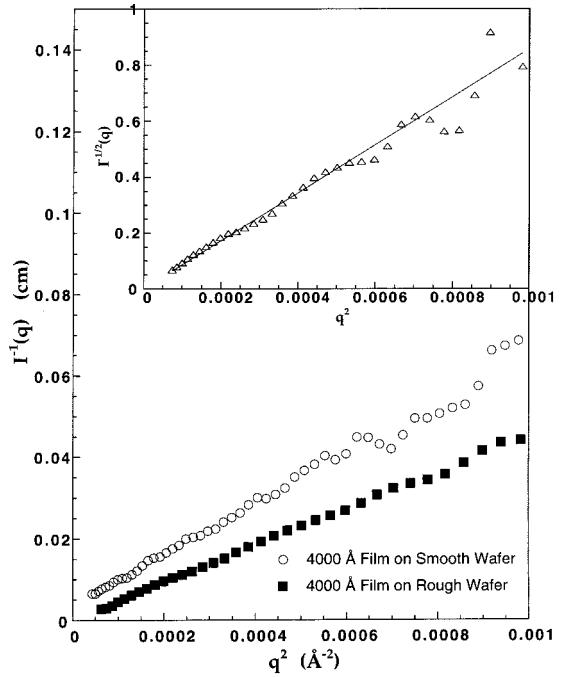

Figure 1. SANS profiles from a smooth (111) Si wafer surface and a rough (100) Si wafer surface. Inset: $I^{-1/2}(q)$ versus q^2 for the residual data from the film on the rough Si(100) wafer after the calculated single-phase scattering has been subtracted.

to the surface, the neutron contrast between the Si and mixture gives rise to scattering characterizing the lateral correlations of the roughness. This scattering is sufficiently large enough to dominate the scattering from the mixture. To further explore the structure induced by the surface roughness, the scattering for the single-phase blend was calculated using the RPA and subtracted from the data for the 4000 Å film on the rough (100) wafer. The remaining scattering data were then plotted as $I^{-1/2}(q)$ versus q^2 (Debye−Bueche analysis[20]). The data are linear over a broad q range, and a correlation length of 1050 Å was obtained (see inset, Figure 1). This correlation length is relatively large (for a SANS measurement) but still smaller than the wavelength of the roughness measured by AFM and optical microscopy (∼1 μm). It is not possible to measure a 1 μm length scale directly by these SANS experiments since the scattering data would be at too small a q value, and as such the measured correlation length probably represents the tail of the roughness distribution. This roughness-induced scattering masks the scattering from the mixture, leading to the conclusion that smooth polished wafers with a roughness well below 30 Å are required for use as substrates in this type of study. A second set of (100) orientation wafers grown by the CZ method were also examined as possible substrates. These wafers were found to exhibit significant small-angle scattering above the open beam background. It has been reported by Livingston et al.[21] that annealing CZ grown silicon single crystals leads to SiO_2 precipitates due to oxygen impurities introduced during crystal growth. Annealing is often done to remove thermal donors generated in a CZ grown crystal as the crystal cools from the growth temperature. Livingston et al. observed enhanced small-angle neutron scattering from annealed crystals and were able to measure R_G = 54 Å for the precipitates in a CZ grown Si single crystal annealed at 750 °C for 72 h. Such excess background scattering from Si wafers can be eliminated by not annealing above 550 °C[22] or by using float zone (FZ) grown crystals which should not develop SiO_2 precipitates.

The SANS data from the polymer films were analyzed using the random phase approximation (RPA).[23−25] The coherent scattering from a binary polymer mixture composed of chains of length N_a and N_b with corresponding volume fractions, ϕ_a and ϕ_b, respectively, is

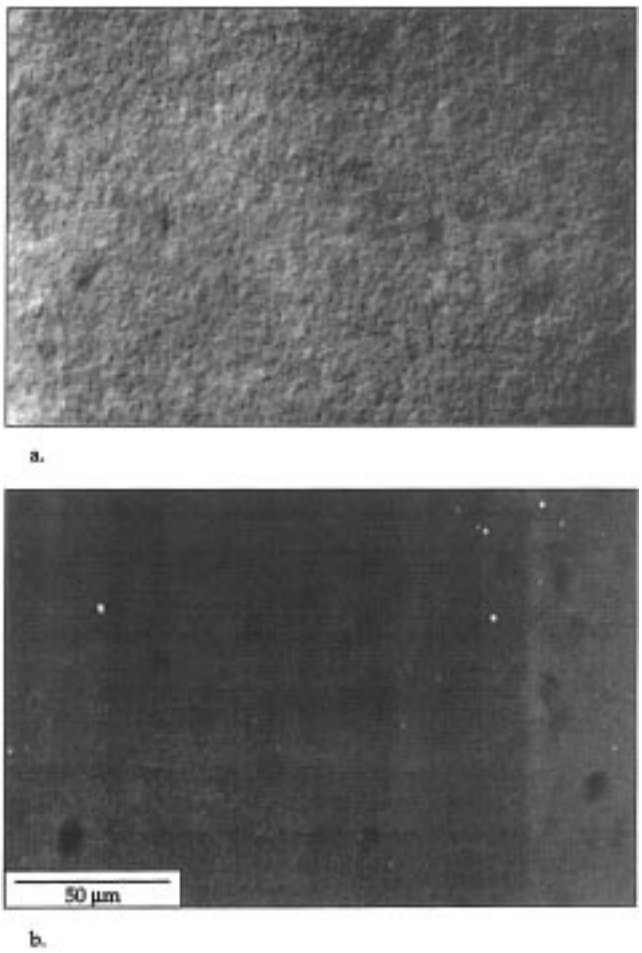

Figure 2. Optical micrographs of (a) a rough (100) Si wafer surface and (b) a smooth (111) Si wafer surface. Both micrographs are on the same scale and were taken using differential interference contrast optical microscopy.

$$\frac{K_n}{I(q)} = \frac{1}{N_a v_a \phi_a P_a(q)} + \frac{1}{N_b v_b \phi_b P_b(q)} - \frac{2\chi}{v_0} \qquad (1)$$

where $K_n = N_A(b_a/v_a - b_b/v_b)^2$ is the neutron contrast factor, N_A is Avogadro's number, v_i is the specific volume, b_i/v_i is the scattering length density of species i, respectively, $v_0 = (v_a v_b)^{1/2}$ is the reference volume, and $P_a(q) = 2(\exp(-X) - 1 + X)/X^2$ is the Debye function with $X = R_G^2 q^2$. Fits of eq 1 to the data provide a measure of χ/v_0 and the statistical step length, l, and allow calculation of the correlation length, ξ, $I(0)$, and R_G ($R_G = Nl^2/6$). If eq 1 is expanded in the limit of small q and rearranged in Ornstein−Zernike format, the correlation length ξ can be calculated using $\xi^2 = l^2[36\phi_a\phi_b(\chi_s - \chi)]^{-1}$ where χ_s is the spinodal χ value ($\chi_s = (1/N_a v_a + 1/N_b v_b)/2$). In the analysis of the experimental data the following parameters were used from the literature:[26−28] v_{PSD} = 100.5 cm^3/mol, v_{PSH} = 99.8 cm^3/mol, and $K_n = 4.16 \times 10^{-3}$ mol/cm^4. Additionally, ϕ_{PSD} = 0.2357, N_{PSD} = 2670, ϕ_{PSH} = 0.7643, and N_{PSH} = 2601. For comparison to the measured data the literature value of $\chi/v_0 = 2.2 \times 10^{-6}$ at 120 °C[5,26] allows the calculation of $I(0)$ = 247 cm^{-1} for this blend.

Results and Discussion

Figure 4 shows the SANS $I(q)$ data as a function of q for all the PSD/PSH thin-film and bulk samples. The data from all of the samples are virtually identical. As expected, the S/N ratio decreases with decreasing film thickness. The signal, S, includes both coherent and incoherent scattering from the sample, while the noise, N, arises from electronic noise and parasitic scattering.

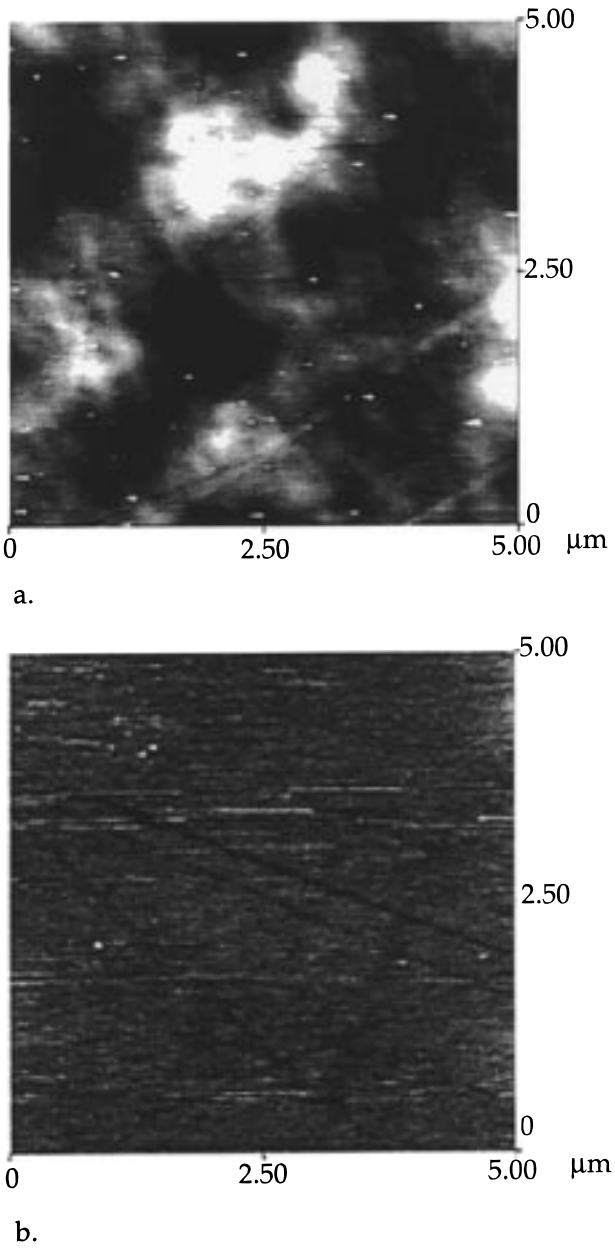

Figure 3. AFM images of (a) a rough (100) Si wafer surface and (b) a smooth (111) Si wafer surface. Both images are on the same scale.

The average S/N ratio at a particular value of the scattering vector for a circularly averaged $I(q)$ versus q data set can be estimated using eq 2 [29,30]

$$\frac{S}{N} = \left(\frac{C_{sam}(t) - C_{emp}(t)}{N_q}\right)^{1/2} \qquad (2)$$

where $C_{sam}(t)$ and $C_{emp}(t)$ are the total detector counts at the specific time t for the sample and empty cell, respectively, and N_q is the number of q intervals ($Nq = 114$ for all data sets). The S/N ratios of the samples are given in Table 3. The S/N ratio decreases with film thickness, and consequently, longer data acquisition times are required for obtaining comparable quality scattering profiles. Nevertheless, even with the relatively low values of S/N shown for the thinnest film, absolute intensities were obtained.

A nonlinear least-squares fit of the RPA model (eq 1) to the data yields the parameters listed in Table 4.

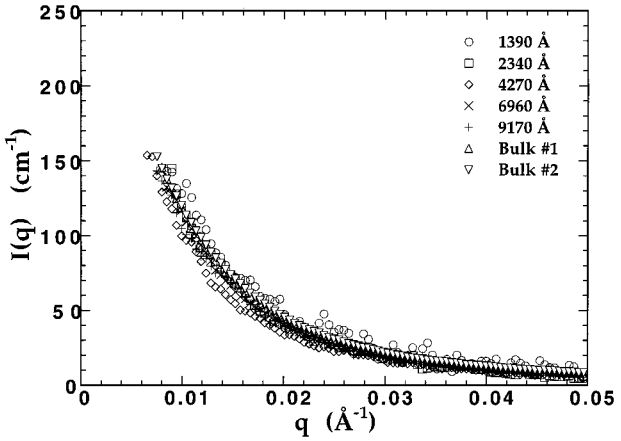

Figure 4. Typical $I(q)$ versus q SANS profiles of samples of all thicknesses examined in this work.

Table 3. Detector Count Rates and Signal-to-Noise Ratios

sample	total detector count rate[b] (counts/s)	S/N[c]
1390[a]	12	18
2340[a]	20	47
4270	38	36
6960	49	45
9170	62	46
bulk no. 1	3218	183
bulk no. 2	3797	199
EMP	28	
EMP[a]	11	

[a] Sample was run with 0.625 in. (1.59 cm) sample aperture. [b] Total detector count rate (background not subtracted). [c] $N_q = 114$ in eq 2 to calculate S/N.

Table 4. Results of RPA Fits

sample	l (Å)	χ/v_0 ($\times 10^7$)	ξ (Å)	$I(0)$ (cm^{-1})
1390	6.4 ± 0.6	7 ± 15	81 ± 7	228 ± 38
2340	6.3 ± 0.4	6 ± 6	79 ± 5	227 ± 20
4270	7.8 ± 0.3	4 ± 6	98 ± 3	221 ± 14
6960	7.4 ± 0.2	14 ± 5	98 ± 3	249 ± 14
9170	7.4 ± 0.3	5 ± 8	93 ± 4	224 ± 18
bulk no. 1	7.0 ± 0.2	7 ± 5	89 ± 2	230 ± 12
bulk no. 2	6.9 ± 0.2	5 ± 5	86 ± 2	225 ± 11

Parts a−d of Figure 5 show the plots of $I(0)$, l, χ/v_0, and ξ as a function of sample thickness, respectively. The error bars were calculated using standard error propagation techniques and correspond to one standard deviation.[31] Within experimental error no dependence of $I(0)$, l, χ/v_0, and ξ on film thickness was found. Therefore, no finite size effects were evident for the PSD/PSH blend, and the thermodynamic and structural properties are identical to the bulk values down to a film thickness of 1390 Å. These results are in contradiction to the preliminary results on PSD/PSH published by Russell et al. and the results on PS/PVME presented by Reich and Cohen. The original work by Russell et al. was on a significantly higher molecular weight blend using Si(100) substrates and the data that may have contained contributions due to surface roughness. In the work by Reich and Cohen on PS/PVME thickness effects were observed for films as thick as 1 μm, but the results varied depending on whether glass or gold was used as a substrate. PS/PVME is also complicated by surface and substrate wetting effects and the fact that PVME is hygroscopic. The results shown here demonstrate that, by proper choice of neutron optics and substrate materials, quantitative SANS can

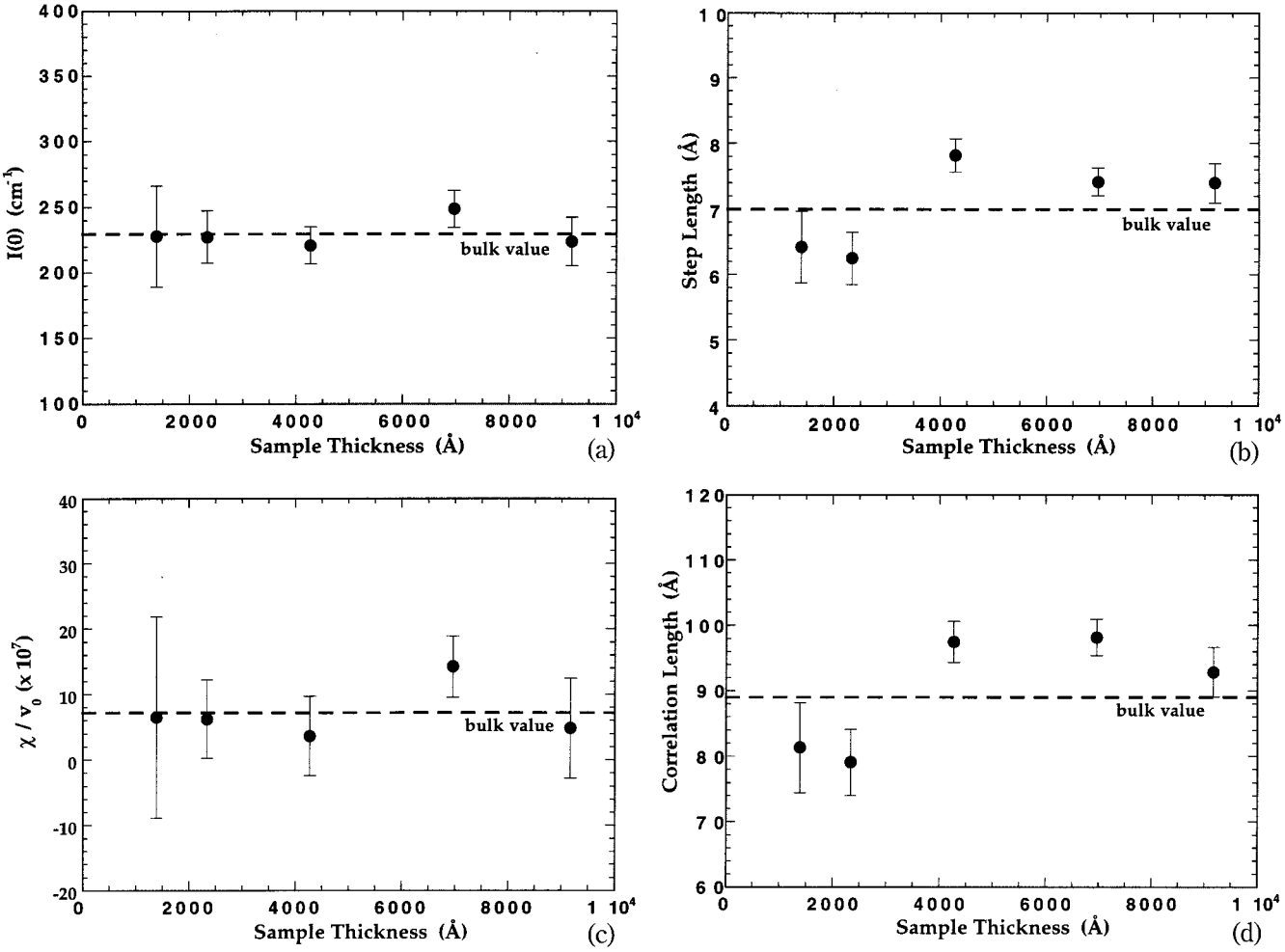

Figure 5. Parameters obtained from RPA fits. Note that the bulk values are denoted in each figure by a straight line: (a) $I(0)$ versus sample thickness, (b) step length versus sample thickness, (c) χ/v_0 versus sample thickness, and (d) correlation length versus sample thickness.

be obtained from very thin polymer films and that changes in the characteristic properties for the model PSD/PSH blend used in this work are small. Although bulk scattering behavior was observed in this work for the thinnest films, finite thickness effects may still be operative for systems close to the phase boundary. The PSD/PSH system chosen in this work was specially selected to be far from the phase boundary. Because of this, the measured scattering will only be sensitive to large shifts in the phase diagram. The amount of this shift can be estimated by noting that for any temperature-dependent property, X (for example, $I(0)$, ξ, ...), that diverges at the spinodal, the scaling behavior is given by

$$X \propto [\chi_S(L) - \chi]^y \propto [1/T_S(L) - 1/T]^y \qquad (3)$$

where the subscripts denote the values of T and χ at the spinodal for a film of thickness L, and y is the scaling exponent for the property of interest. If a 20% change in $I(0)$ is taken as the minimum observable change within errors, then a 20 °C shift in the phase diagram would be required. Consequently, any changes less than this would not be observable. Sensitivity of the experiment to shifts in the phase diagram can be enhanced by performing experiments closer to the spinodal point and will be the subject of future experiments.

It has been observed that the density of a polymer film thinner than the chain end-to-end distance decreases with decreasing film thickness.[32−34] Orts et al.[32] reported that a decrease in density of ultrathin polystyrene films with decreasing film thickness was observed though the density variation could not be determined quantitatively. The question arises as to whether a change in density of the polystyrene as the film thickness decreases would affect the results of the fit of the data reported in this work to the RPA equation (eq 1). Varying the specific volumes of PSD and PSH from the literature values[27,28] by ±5% and refitting the data does not change the values of $I(0)$, χ, ξ, and l significantly. (The relative changes in these parameters are less than 1%.)

A final issue that needs to be addressed is the role of surface segregation on the scattering obtained from thin films of polymer blends. The preferential segregation of one component to an interface will cause a reduction in the concentration of that component in the interior of the film. This would cause a shift in the phase separation temperature due to a composition change and, consequently, a change in the scattering. This effect has no relation to shifts in the spinodal temperature due to finite size effects. Past work of Kramer and co-workers[35] has suggested that the deuterated component from an isotopic polystyrene mixture with equal chain length polymers would partition to the air

surface, since it has a lower surface free energy. The situation at the Si interface is far less clear and is affected by the nature of the Si surface, i.e., if it is the native oxide or if it is passivated with HF.[36] If it is assumed that the segregation at both interfaces (air and substrate) is similar to that predicted at the air surface by the mean-field theory of Schmidt and Binder[37] with surface energy parameters from ref 35, the maximum shift in the phase separation temperature can be estimated. The film was modeled by layers of homogeneous composition parallel to the film surface with incremental changes in the composition between layers used to approximate the composition profile normal to the surface as predicted by Schmidt and Binder. The scattering from each layer was assumed to be given by eq 1, and the calculated scattering from each layer was summed incoherently. The scattering calculated by this method was found to deviate less than 1% relative to that calculated for a film exhibiting no surface segregation effects. Consequently, surface segregation effects cannot be considered significant in these studies.

Conclusions

In summary, it has been demonstrated that SANS can be performed to obtain quantitative intensities on single films of a PSD/PSH polymer blend film supported on a Si wafer substrate down to a film thickness of 1390 Å. This work demonstrates the feasibility of experiments on a new class of polymer sample with quantities of material as small as 100 μg. Analysis of the data has shown that the measured scattering is consistent with the bulk, indicating that, for the molecular weights and composition examined in this paper, finite size effects on the thermodynamics of the mixture were not observable. In addition, surface segregation effects are not expected to alter the scattering significantly. Future studies are in progress to test the feasibility of stacking of multiple films to extend the technique to thinner films and on higher molecular weight mixtures to examine finite size effects on the thermodynamics and chain conformation properties.

Acknowledgment. We acknowledge the support of the National Institute of Standards and Technology, U.S. Department of Commerce, and the National Science Foundation, through Agreement No. DMR-9423101, in providing the neutron research facilities used in this work. Financial support from the American Chemical Society, Petroleum Research Fund [S.K.K.], the National Science Foundation [CTS-9704907, S.K.K.], the Department of Energy, Office of Basic Energy Sciences [DE-FG03-88ER45375, T.P.R.], and the Department of Commerce [7NANB7H0055, R.M.B., D.L.H.] is gratefully acknowledged. We thank Drs. Tania Slawecki and Alamgir Karim at the NIST for their assistance during these experiments and Mr. Lee Rockford at the University of Massachusetts for the AFM measurements.

References and Notes

(1) Higgins, J. S.; Benoit, H. C. *Polymers and Neutron Scattering*; Oxford: New York, 1994.
(2) Lovesey, S. W. *Theory of Neutron Scattering from Condensed Matter*; Oxford: New York, 1984.
(3) Feigin, L. A.; Svergun, D. I. *Structure Analysis by Small-Angle X-Ray and Neutron Scattering*; Plenum: New York, 1987.
(4) Russell, T. P.; Lambooy, P.; Barker, J. G.; Gallagher, P.; Satija, S. K.; Kellogg, G. J.; Mayes, A. M. *Macromolecules* **1995**, *28*, 787.
(5) Londono, J. D.; Narten, A. H.; Wignall, G. D.; Honnell, K. G.; Hsieh, E. T.; Johnson, T. W.; Bates, F. S. *Macromolecules* **1994**, *27*, 2864.
(6) Reich, S.; Cohen, Y. *J. Polym. Sci., Polym. Phys. Ed.* **1981**, *19*, 1255.
(7) Kumar, S. K.; Tang, H.; Szleifer, I. *Mol. Phys.* **1994**, *81*, 867. Tang, H.; Szleifer, I.; Kumar, S. K. *J. Chem. Phys.* **1994**, *100*, 5367.
(8) Rouault, Y.; Baschnagel, J.; Binder, K. *J. Stat. Phys.* **1995**, *80*, 1009.
(9) Cifra, P.; Karasz, F. E.; Macknight, W. J. *J. Polym. Sci., Part B: Polym. Phys.* **1992**, *30*, 1401.
(10) Flebbe, T.; Dunweg, B.; Binder, K. *J. Phys. II* **1996**, *6*, 667.
(11) Wignall, G. D. In *Encyclopedia of Polymer Science and Engineering*; Mark, H., et al., Eds.; John Wiley & Sons: New York, 1978; Vol. 10, p 121.
(12) Zabel, H.; Robinson, I. K. *Surface X-Ray and Neutron Scattering*; Springer-Verlag: New York, 1992.
(13) Bienfait, M.; Gay, J. M. *X-Ray and Neutron Scattering from Surfaces and Thin Films*; Colloque De Physique: Paris, 1989.
(14) Baker, S. M.; Smith, G. S.; Pynn, R.; Butler, P. D.; Hayter, J. B.; Hamilton, W. A.; Magid, L. J. *Rev. Sci. Instrum.* **1994**, *65*, 412.
(15) Hamilton, W. A.; Butler, P. D.; Baker, S. M.; Smith, G. S.; Hayter, J. B.; Magid, L. J.; Pynn, R. *Phys. Rev. Lett.* **1994**, *72*, 2219.
(16) Bates, F. S.; Wignall, G. D.; Koehler, W. C. *Phys. Rev. Lett.* **1985**, *55*, 2425.
(17) Taylor, B. N., et al., Eds. *J. Res. NIST* **1993**, *98*, 31.
(18) MacGillavry, C. H.; Rieck, G. D. *International Tables of Crystallography*; Kynoch Press: Birmingham, England, 1962; Vol. III.
(19) Cold Neutron Research Facility at the National Institute of Standards and Technology, NG3 and NG7 30-Meter SANS Instruments Data Acquisition Manual, 1996.
(20) Debye, P.; Bueche, A. M. *J. Appl. Phys.* **1949**, *20*, 518.
(21) Livingston, F. M.; Messoloras, S.; Newman, R. C.; Pike, B. C.; Stewart, R. J.; Binns, M. J.; Brown, W. P.; Wilkes, J. G. *J. Phys. (Paris)* **1984**, *C17*, 6253.
(22) Schneider, J. R.; Goncalves, O. D.; Rollason, A. J.; Bonse, U.; Lauer, J.; Zulehner, W. *Nucl. Instrum. Methods* **1988**, *B29*, 661.
(23) de Gennes, P. G. *J. Phys. (Paris)* **1970**, *31*, 235.
(24) Hadziioannou, G.; Stein, R. S. *Macromolecules* **1984**, *17*, 567.
(25) Warner, M.; Higgins, J. S.; Carter, A. J. *Macromolecules* **1983**, *16*, 1931.
(26) Hammouda, B.; Briber, R. M.; Bauer, B. J. *Polymer* **1992**, *33*, 1785.
(27) Yang, H.; Shibayama, M.; Stein, R. S.; Shimizu, N.; Hashimoto, T. *Macromolecules* **1986**, *19*, 1667.
(28) Shibayama, M.; Yang, H.; Stein, R. S.; Han, C. C. *Macromolecules* **1985**, *18*, 2179.
(29) Whalen, A. D. *Detection of Signals in Noise*; Academic: New York, 1971.
(30) Papoulis, A. *Signal Analysis*; McGraw-Hill: New York, 1977.
(31) Bowker, A. H.; Lieberman, G. J. *Engineering Statistics*; Prentice-Hall: Englewood Cliffs, NJ, 1972.
(32) Orts, W. J.; van Zanten, J. H.; Wu, W.-L.; Satija, S. K. *Phys. Rev. Lett.* **1993**, *71*, 867.
(33) Wu, W.-L.; van Zanten, J. H.; Orts, W. J. *Macromolecules* **1995**, *28*, 771.
(34) Reiter, G. *Macromolecules* **1994**, *27*, 3046.
(35) Jones, R. A. L.; Kramer, E. J.; Rafailovich, M. H.; Sokolov, J.; Schwarz, S. A. *Phys. Rev. Lett.* **1988**, *62*, 2801.
(36) Hariharan, A.; Kumar, S. K.; Rafailovich, M. H.; Sokolov, J.; Schwarz, S.; Russell, T. P. *J. Chem. Phys.* **1993**, *99*, 656.
(37) Schmidt, I.; Binder, K. *J. Phys. Paris, C3* **1985**, *46*, 1631.

MA980733S